Gapless behavior in a two-leg spin ladder with bond randomness

Yu Tominaga,[1] Itsuki Shimamura,[1] Takanori Kida,[2] Masayuki Hagiwara,[2] Koji Araki,[3] Yuko Hosokoshi,[1] Yoshiki Iwasaki,[4,5] and Hironori Yamaguchi[1,5]

[1]*Department of Physics, Osaka Metropolitan University, Osaka 599-8531, Japan*

[2]*Center for Advanced High Magnetic Field Science (AHMF), Graduate School of Science, Osaka University, Osaka 560-0043, Japan*

[3]*Department of Applied Physics, National Defense Academy, Kanagawa 239-8686, Japan*

[4]*Department of Physics, College of Humanities and Sciences, Nihon University, Tokyo 156-8550, Japan*

[5]*Innovative Quantum Material Center (IQMC), Osaka Metropolitan University, Osaka 599-8531, Japan*

(Received 23 November 2024; revised 21 February 2025; accepted 10 April 2025; published 18 April 2025)

We successfully synthesized $[Cu_2(AcO)_4(p-Py-V-p-F)_2] \cdot 4CHCl_3$, a verdazyl-based complex with a paddlewheel structure comprising two Cu atoms, which induces strong antiferromagnetic (AF) exchange interactions between Cu spins, generating a nonmagnetic singlet state at low temperatures. Two primary exchange interactions between radical spins generate a spin-1/2 AF two-leg ladder. In addition, two possible positional configurations of the F atom in the complex create four different overlap patterns of molecular orbitals, introducing bond randomness in the spin ladder. The observed experimental behaviors, such as the Curie tail in the magnetic susceptibility and the gapless gradual increase in the magnetization curve, are attributed to a broad distribution of excitation energies and a few orphan spins in the random-singlet (RS) state that are stabilized by bond randomness. The low-temperature specific heat exhibits a temperature dependence with $\propto 1/|\ln T|^3$, demonstrating the formation of the RS state in unfrustrated systems. We also consider the effect of restricted patterns of exchange interactions and one-dimensional nature of the system on the RS state.

DOI: 10.1103/PhysRevB.111.134430

I. INTRODUCTION

Spin ladders, which comprise coupled spin chains, are crucial for investigating low-dimensional quantum systems, bridging one-dimensional (1D) chains and two-dimensional lattices. These systems provide insights into phenomena driven by the interplay between dimensionality and quantum fluctuations, with potential relevance to high-temperature superconductivity [1,2]. The spin-1/2 antiferromagnetic (AF) two-leg ladder, in particular, serves as a fundamental model, revealing the complex physics of ladder systems. In these systems, spins along the rungs form singlet pairs, leading to a gapped ground state. When a magnetic field is applied, the spin gap gradually closes and the system transitions into a Tomonaga-Luttinger liquid (TLL) phase—a gapless quantum critical state. Numerous spin ladder compounds have been experimentally identified and extensively studied, consistently confirming the predicted quantum behaviors, including the closing of the spin gap and emergence of the TLL phase [3–6].

Randomness plays a crucial role in determining the physical properties of condensed matter systems. Even a small amount of disorder can notably alter the quantum behavior, leading to the emergence of novel quantum phases and critical phenomena. This disorder can have profound effects on various material properties, including transport phenomena, magnetic ordering, and quantum phase transitions. The effect of randomness is particularly prominent in low-dimensional quantum spin systems, which are highly susceptible to quantum fluctuations and disorder. These systems give rise to the gapless quantum state known as the random singlet (RS) state. In the last century, extensive theoretical studies have investigated the ground state of the 1D spin-1/2 chain with randomness, identifying it as the unfrustrated RS state [7–10]. For the frustrated case, recent numerical studies on various spin-1/2 systems have shown that the introduction of randomness universally induces the RS state, referred to as the frustrated RS state [11–15]. Moreover, a quantum phase transition between the unfrustrated and frustrated RS states has been identified, demonstrating that these two RS states exhibit qualitatively different low-temperature behavior [16]. For spin ladders, numerous studies have explored site randomness and its influence on quantum phases and critical phenomena [17–19]. However, bond randomness, where disorder affects the interaction strength between spins, remains less studied. While theoretical predictions suggest that bond randomness in spin-1/2 AF two-leg ladders can significantly alter quantum phases and quasiparticle excitations [20–22], experimental realizations of bond randomness are scarce and its effects have not been thoroughly investigated.

We developed a unique class of materials, verdazyl-based quantum organic materials (V-QOM), which offer exceptional flexibility in molecular design and precise control over spin interactions. Previous studies with V-QOM have demonstrated the realization of unconventional spin lattices that are yet to be generated in traditional inorganic materials [23–27]. By leveraging the properties of V-QOM, we successfully introduced randomness in exchange interactions by generating regioisomers that randomly align within the crystals. This led to the realization of a RS state in a spin-1/2 honeycomb lattice, marking a significant advancement in the understanding of quantum phenomena induced by bond randomness [28]. These developments represent a

 ©2025 American Physical Society

robust basis for exploring mechanisms underlying quantum criticality.

In this study, we synthesized $[Cu_2(AcO)_4(p-Py-V-p-F)_2]\cdot 4CHCl_3$ ($AcO = CH_3COO^{-1}$, $p-Py-V-p$-F = 3-(4-pyridinyl)-1-(4-fluorophenyl)-5-phenylverdazyl), a verdazyl-based complex. The four bridging acetates and two $p-Py-V-p$-F ligands formed a paddlewheel structure, where the strong AF exchange interactions between Cu spins created a spin-1/2 AF dimer, generating a nonmagnetic singlet state at low temperatures. We identified two primary exchange interactions between the radical spins that generated the spin-1/2 AF two-leg ladder. Two possible positional configurations for the F atom in the complex introduced bond randomness in the spin ladder, stabilizing the RS state. Magnetic properties revealed AF gapless behavior with low paramagnetic contributions in the RS state. The low-temperature specific heat exhibited the $1/|\ln T|^3$ behavior predicted for the unfrustrated RS state. We also examined the effect of restricted patterns of exchange interactions and 1D nature of the systems on the RS state.

II. EXPERIMENTAL

We synthesized p-Py-V-p-F via the conventional procedure for producing the verdazyl radical [29]. A solution of $Cu(AcO)_2\cdot H_2O$ (79.9 mg, 0.40 mmol) in 7 ml ethanol was slowly added to a solution of p-Py-V-p-F (132.9 mg, 0.40 mmol) in 8 ml of CH_2Cl_2 and stirred for 30 min. A dark-green crystalline solid of $[Cu_2(AcO)_4(p-Py-V-p-F)_2]$ was separated by filtration. Single crystals were obtained via recrystallization from $CHCl_3$ at 10 °C.

The x-ray intensity data were collected using a Rigaku XtaLAB Synergy-S instrument. The crystal structures was determined using a direct method using SIR2004 and refined using the SHELXL97 crystal structure refinement program. Anisotropic and isotropic thermal parameters were employed for nonhydrogen and hydrogen atoms, respectively, during the structure refinement. The hydrogen atoms were positioned at their calculated ideal positions. Magnetization measurements were conducted using a commercial superconducting quantum interference device magnetometer (MPMS, Quantum Design). The experimental results were corrected by considering the diamagnetic contributions calculated using Pascal's method. High-field magnetization in pulsed magnetic fields was measured using a nondestructive pulse magnet at AHMF, Osaka University. Specific heat measurements were performed using a commercial calorimeter (PPMS, Quantum Design) employing a thermal relaxation method. All the experiments utilized small, randomly oriented single crystals.

Molecular orbital (MO) calculations were performed using the UB3LYP method. The basis sets are 6-31G (intermolecule) and 6-31G(d, p) (intramolecule). All calculations were performed using the GAUSSIAN09 software package. The convergence criterion was set at 10^{-8} hartrees. We employed a conventional evaluation scheme to estimate the intermolecular exchange interactions in the molecular pairs [30].

The quantum Monte Carlo code is based on the directed loop algorithm in the stochastic series expansion representation [31]. The calculations were performed for $N = 256$ under the periodic boundary condition, where N denotes the system size. All calculations were carried out using the ALPS application [32,33].

TABLE I. Crystallographic data of $[Cu_2(AcO)_4(p-Py-V-p-F)_2]\cdot 4CHCl_3$.

Formula	$C_{50}H_{44}Cu_2Cl_{12}F_2N_{10}O_8$
Crystal system	Monoclinic
Space group	$P2_1/n$
Temperature (K)	100
a (Å)	19.0001(5)
b (Å)	9.5444(2)
c (Å)	19.0221(4)
β (degrees)	114.183(3)
V (Å^3)	3146.84(12)
Z	2
D_{calc} (g cm^{-3})	1.587
Total reflections	3621
Reflection used	3064
Parameters refined	391
$R\ [I > 2\sigma(I)]$	0.0561
$R_w\ [I > 2\sigma(I)]$	0.1511
Goodness of fit	1.041
CCDC	2405110

III. RESULTS

A. Crystal structure and spin model of the complex

The crystallographic parameters of $[Cu_2(AcO)_4(p-Py-V-p-F)_2]\cdot 4CHCl_3$ are provided in Table I. Figure 1(a) shows the molecular structure, wherein the verdazyl radical, p-Py-V, and Cu^{2+} have a spin value of 1/2. Table II lists the bond lengths and angles of the Cu atoms. The four bridging acetates and two $p-Py-V-p$-F ligands form a distorted square pyramidal geometry around the Cu atoms—typical of Cu^{2+} carboxylate dimers—which is known as the paddlewheel structure. An inversion center located at the Cu_2 core, and the Cu–Cu distance (2.61 Å) is comparable with those of the other paddlewheel structures [34,35]. A Cu-Cu bond is not formed due to the lack of properly oriented orbitals for overlap, resulting in a five-coordinated square pyramid. Two possible positional configurations are observed for the F atom [Fig. 1(a)], with rations of 0.786(9) and 0.214(9) for

TABLE II. Bond lengths (Å) and angles (°) related to the Cu atoms in $[Cu_2(AcO)_4(p-Py-V-p-F)_2]\cdot 4CHCl_3$.

Cu1–N1	2.16	N1–Cu1–O1	95.6
Cu1–O1	1.96	O1–Cu1–O3	169.3
Cu1–O2	1.98	O3–Cu1–N1	95.0
Cu1–O3	1.97	O1–Cu1–O2	89.6
Cu1–O4	1.96	O2–Cu1–O3	89.0
Cu1–Cu2	2.61	O3–Cu1–O4	90.4
		O4–Cu1–O1	89.1
		N1–Cu1–O2	94.5
		O2–Cu1–O4	169.3
		O4–Cu1–N1	96.2

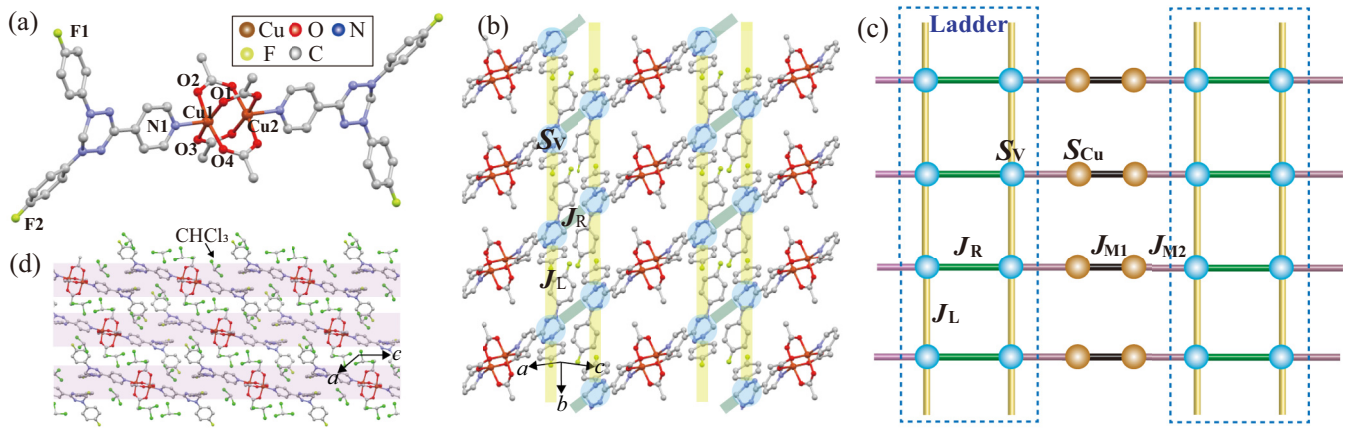

FIG. 1. (a) Molecular structure of $[Cu_2(AcO)_4(p-Py-V-p-F)_2]$, which causes intramolecular exchange interactions J_{M1} between the Cu spins and J_{M2} between the radical and Cu spins. The hydrogen atoms have been omitted for clarity. (b) The 2D crystal structure and (c) corresponding spin-1/2 2D lattice with two different spin sites, S_V and S_{Cu}. The broken lines indicate the effective spin ladder. (d) Crystal structure in the *ac* plane. The thick lines represent the 2D spin planes.

F1 and F2, respectively, as determined by x-ray single crystal analysis. These two configurations introduced randomness in the MO overlap. Regarding the spin density distribution in the radicals, MO calculations showed that ∼61 % of the total spin density was localized on the central ring consisting of four N atoms, while each fluorophenyl ring directly attached to the central N atom contributed ∼16 % of the spin density. Dominant exchange interactions were identified through MO calculations. Regarding intramolecular interactions, the AF exchange interactions between the Cu spins in the paddle-wheel structure and those between the radical spin and Cu spin were evaluated to be $J_{M1}/k_B = 572$ K and $J_{M2}/k_B = 4.9$ K, respectively, defined within the Heisenberg spin Hamiltonian, given by $\mathcal{H} = J_n \sum_{<i,j>} S_i \cdot S_j$. Given that MO calculations tend to overestimate the intramolecular interactions with transition metals, the actual values are expected to be smaller [36,37]. Regarding intermolecular interactions, two primary exchange interactions, J_R and J_L, generated a spin-1/2 two-leg ladder along the *b* axis, as depicted in Fig. 1(b). Thus, the interactions J_{M1}, J_{M2}, J_R, and J_L from a spin-1/2 two-dimensional (2D) lattice with two distinct spin sites, S_V and S_{Cu} [Fig. 1(c)]. Due to the presence of nonmagnetic $CHCl_3$ molecules between the 2D structures, exchange interactions between the spin lattices are expected to be weak enough to be neglected in this study [Fig. 1(d)].

We also evaluated the values of J_R and J_L, which correspond to the rung and leg interactions in the spin ladder, respectively. The molecular pairs associated with J_R and J_L are related by inversion symmetry and translational symmetry along the *b* axis, respectively, as depicted in Figs. 2(a) and 2(b). Since the actual radicals have either F1 or F2, each overlap of the MOs associated with J_R and J_L has four radical pairing patterns with different F positions, i.e., F1-F1, F1-F2, F2-F1, and F2-F2. The possibilities of these pairing patterns and corresponding evaluations of J_R and J_L are summarized in Table III. Notably, J_R strongly depends on the F position, and the pairs F1-F2 and F2-F1 are equivalent due to the inversion center between the radicals. In contrast, J_L exhibits weak dependence on the F position, although the uniform bond is distorted by randomness in the MO overlap.

B. Magnetic and thermodynamic properties

Figure 3(a) shows the temperature dependence of the magnetic susceptibility (χ) of the complex at 0.1 T, showing a broad peak at ∼14 K. The upturn below ∼4 K suggests paramagnetic contribution. Assuming conventional paramagnetic behavior C_{para}/T, where C_{para} is the Curie constant of paramagnetic spins, the paramagnetic contribution is found to be in the range of 3%–5% of all spins. This relatively large paramagnetic contribution could not be reduced by purification processes that have been effective in other verdazyl-based compounds. The temperature dependence of χT, as shown in Fig. 3(b), reveals a two-step decrease as the temperature decreases. The initial decrease, down to ∼100 K, is attributed to the formation of a spin-1/2 singlet dimer of S_{Cu} resulting from the strong AF interaction J_{M1}. Further decrease at low temperatures reflects AF behavior originating from residual radical spins forming the spin-1/2 ladder. We calculated the magnetic susceptibility of the spin-1/2 AF dimer of S_{Cu} and fitted it to the experimental χT data above ∼100 K. The calculated value was shifted up by 0.72 emu K/mol, corresponding to a Curie constant for spin-1/2 systems with $g = 2$ and a radical purity of 96%, when accounting for the contribution of S_V [Fig. 3(b)]. The experimental behavior was

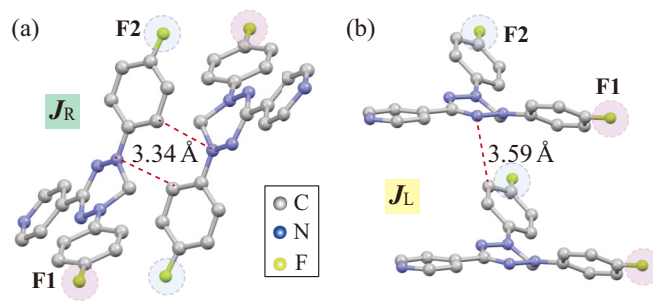

FIG. 2. Intermolecular radical pairs of $[Cu_2(AcO)_4(p-Py-V-p-F)_2] \cdot 4CHCl_3$ associated with exchange interactions (a) J_R and (b) J_L. Hydrogen atoms and $Cu_2(AcO)_4$ are omitted for clarity. The dashed lines indicate N-C short contacts.

TABLE III. Possible radical pair patterns with different F positions and the values of J_R and J_L evaluated from MO calculations.

Pattern	Possibility	J_R/k_B (K)	J_L/k_B (K)
F1–F1	0.618	8.0	1.6
F1–F2	0.168	5.8	1.6
F2–F1	0.168	5.8	2.0
F2–F2	0.046	3.8	2.0

then explained using $J_{M1}/k_B = 446(3)$ K and $g = 2.33(1)$, consistent with previously reported values for the paddlewheel structure [38–41].

Figure 3(c) shows the magnetization curve of the complex under a pulsed magnetic field applied at 1.4 K. The magnetization increases gradually up to ∼10 T, showing gapless behavior, and then rises sharply toward ∼30 T. The value of ∼2.0 μ_B/f.u. suggests full polarization of S_V with an isotropic g value of 2.0, corresponding to the saturation of the spin ladder. A slight paramagnetic contribution observed below 5 T, resembling the Brillouin function and consistent with the low-temperature upturn of χ. In typical spin ladders forming a gapped singlet state, the energy gap decreases under applied magnetic field, leading to a quantum phase transition to the TLL phase with a sharp increase in the magnetization [42–44]. However, the observed magnetization behavior deviates from this quantum critical behavior.

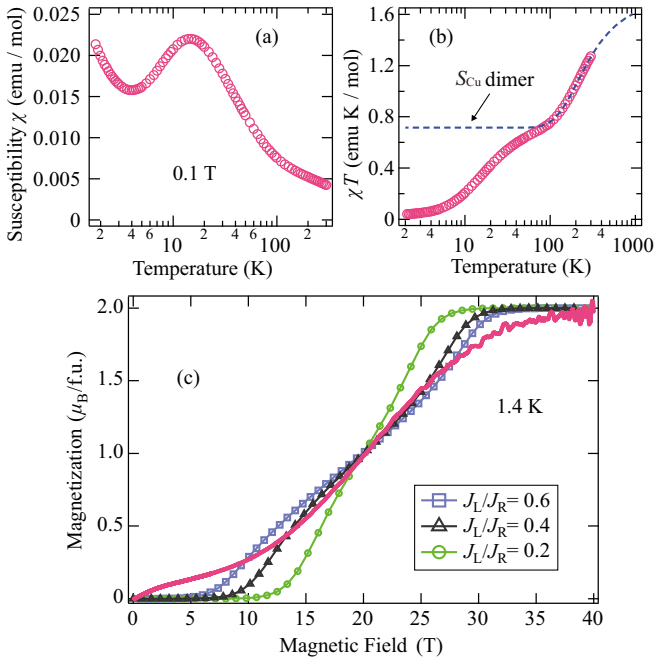

FIG. 3. Temperature dependence of (a) the magnetic susceptibility ($\chi = M/H$) and (b) χT of $[Cu_2(AcO)_4(p-Py-V-p-F)_2] \cdot 4CHCl_3$ at 0.1 T. The broken line represents the result calculated for a spin-1/2 AF dimer of S_{Cu} via J_{M1}. (c) The magnetization curve of $[Cu_2(AcO)_4(p-Py-V-p-F)_2] \cdot 4CHCl_3$ at 1.4 K under applied pulsed magnetic fields. The solid lines show calculated magnetization curves at 1.4 K for the spin-1/2 ladder with the representative values of J_L/J_R.

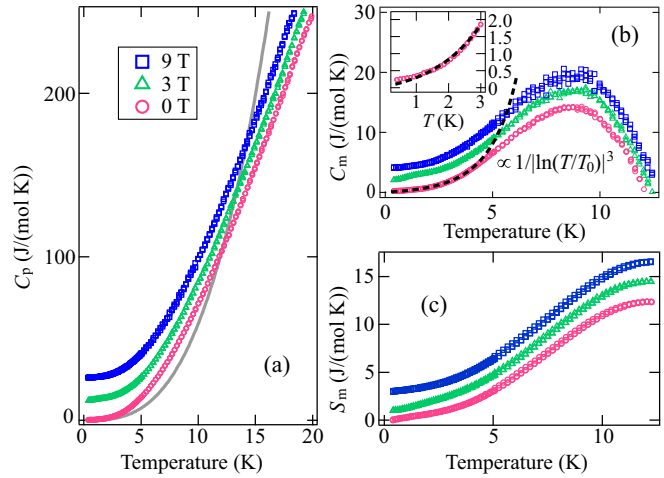

FIG. 4. (a) Temperature dependence of the specific heat C_p of $[Cu_2(AcO)_4(p-Py-V-p-F)_2] \cdot 4CHCl_3$. The values at 3 and 9 T have been shifted up by 12 and 26 J/mol K, respectively. The solid line indicates the lattice contribution by assuming Debye's T^3 law. (b) Temperature dependence of the magnetic specific heat C_m evaluated by subtracting the lattice contribution. The values at 3 and 9 T have been shifted up by 2 and 4 J/mol K, respectively. The broken line indicates the $1/|\ln T/T_0|^3$ behavior. The inset shows the expansion of the low-temperature region at 0 T. (c) Magnetic entropy S_m obtained by integrating C_m/T. Here, we shifted the values at 3 and 9 T upward by 1 and 3 J/mol K, respectively.

The temperature dependence of specific heat C_p is shown in Fig. 4(a). There is no peak showing phase transition toward magnetic long-range order. We assumed the lattice contribution of C_p to be αT^3, corresponding to Debye's T^3 law for the low-temperature region, which is confirmed to be effective below ∼10 K in verdazyl-based compounds [23,44]. We then evaluated the magnetic specific heat C_m by subtracting the lattice contribution of C_p, as shown in Fig. 4(b). The magnetic contributions contain inaccuracies in higher temperature regions, leading to the negative values above ∼12 K. We determined the value of α such that the magnetic entropy S_m, which was obtained by integrating C_m/T, exhibited asymptotic behavior near the broad peak temperature in χ below which the AF correlation was expected to emerge appreciably. The obtained value $\alpha = 0.059$, corresponding to a Debye temperature of 32 K, was close to that of similar verdazyl-based complex [45]. Furthermore, the entropy change in the low-temperature region was close to the total magnetic entropy associated with a spin ladder composed of S_V (11.5; $2R\ln 2$). The C_m exhibited a broad peak, which was almost unchanged by the application of magnetic fields with magnitudes of up to 9 T. This magnetic-field-insensitive behavior demonstrated that the broad peak did not arise from a Schottky-type behavior related to an energy gap; rather, it resulted from the development of AF correlations in the spin-1/2 ladder. Considering the energy scale observed in the magnetization curve, the change in entropy induced by the application of a magnetic field is expected to be significant above ∼10 T, leading to a corresponding change in the specific heat values.

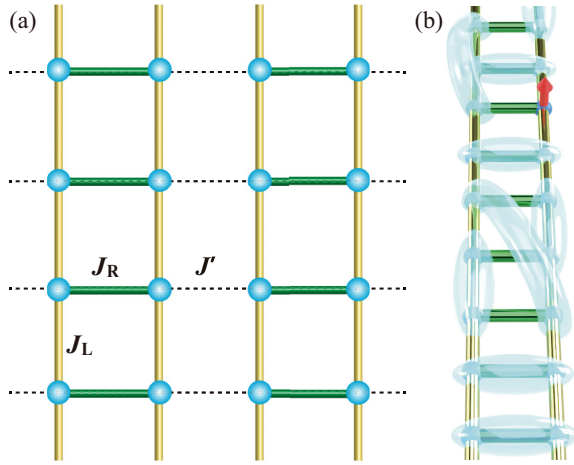

FIG. 5. (a) Two-leg spin ladder in $[Cu_2(AcO)_4(p-Py-V-p-F)_2]\cdot 4CHCl_3$. The effective inter-ladder interaction J' occurs through the triplet excited states of the S_{Cu} dimer. (b) RS state in the studied spin ladder. Entangled singlet dimers are indicated by ovals that cover two lattice sites. The dimers can be formed in a spatially random manner not only between neighboring sites but also between distant sites through higher-order interactions. The red arrow represents an unpaired orphan spin.

IV. DISCUSSION

We also examined the ground state of the spin model. The Cu spins coupled by strong AF J_{M1} interactions formed a nonmagnetic singlet dimer at low temperatures. Consequently, an exchange interaction J' through the triplet excited states of the J_{M1} dimer was expected to occur between the radical spins, as depicted in Fig. 5(a). Assuming $T \ll J_{M1}/k_B$, a second-order perturbation treatment of the exchange interaction between S_V and S_{Cu}—i.e., J_{M2}—yielded $J' = J_{M2}^2/2J_{M1}$ [46,47]. Considering $J_{M1}/k_B = 446$ K determined from the magnetization analysis and $J_{M2}/k_B = 4.9$ K determined from MO calculations, we estimated the value of J' to be <0.1 K, which was negligible at our experimental temperatures. Hence, the spin model in the low-temperature region can be regarded as a spin-1/2 AF two-leg ladder composed of S_V.

Further, we discuss the effects of bond randomness in the prepared spin ladder. Bond randomness is expected to stabilize the RS state, wherein singlet dimers of varying strengths are formed in a spatially random manner [7]. Because the exchange interactions are randomly distributed in the RS state, the binding energies of the singlet dimers have a broad distribution, showing gapless behavior. For magnetic susceptibility, Curie-like diverging components appear in the low-temperature region, reflecting paramagnetic contribution from some unpaired orphan spins [11,13]. For the prepared system, we observed the Curie tail in χ, which suggests the existence of orphan spins specific to the RS state. The evaluated amount of the paramagnetic contribution is indeed larger than those evaluated in other verdazyl-based compounds, which originate only from the lattice defects [23,24]. Because of the lattice symmetry of the spin ladder, a rung singlet alone, i.e., $J_R > J_L$, cannot generate the orphan spins. Therefore, the actual values of J_R and J_L apparently differ somewhat from the MO evaluations presented in Table III, which suggests that $J_R < J_L$ partially exists. In this case, J_L allows the formation of singlet dimers, which yields the orphan spins, as illustrated in Fig. 5(b).

For the magnetization curve, the RS state is predicted to exhibit a near-linear behavior, reflecting the wide distribution of excitation energies [11]. However, our experimental result for the magnetization curve reveal a gapless but nonlinear behavior. We attribute this difference to the effect of randomness, which is limited by the characteristics of the present system. Bond randomness is limited to three J_R patterns and two J_L patterns, and the single dimension of the lattice restricts the spatial distribution. Consequently, although the excited state is gapless, the density of states depends strongly on the probability of existence of each exchange interaction. The observed large increase in the magnetization above ~10 T is considered to be due to the J_R interaction (F1-F1), which has the highest probability of existence.

To examine accurate energy scale of the present model, which strongly reflects the values of J_R (F1-F1), we calculated the magnetization curves by considering J_L/J_R. Figure 3(b) shows the calculated results for representative values of J_L/J_R, demonstrating the difference from the experimental behavior. The magnetization curve for each J_L/J_R was scaled to have the same energy scale by adjusting the value of J_R. As a result, identical intermediate fields toward saturation were obtained. Consequently, the values of J_R/k_B were determined as 24 K ($J_L/J_R = 0.2$), 21 K ($J_L/J_R = 0.4$), and 18 K ($J_L/J_R = 0.6$). Although quantitative comparison with the experimental results is unreliable due to the randomness effect, we can roughly estimate the actual value of J_R (F1-F1) to be ~20 K, indicating the underestimation of the MO evaluations. A relatively large difference from the MO evaluation may be related to the presence of the randomness in the molecular packing.

For the specific heat, numerical studies predict that a qualitative difference between unfrustrated and frustrated RS states appears in the low-temperature region [16]. The unfrustrated RS state, which corresponds to the present model, exhibits a specific heat behavior proportional to $1/|\ln T/T_0|^3$, while the frustrated RS state follows a T-linear behavior. Experimentally, the magnetic specific heat shows a clear nonlinear behavior and is well reproduced by the $1/|\ln T/T_0|^3$ fit for $T <$ 4 K, as shown in Fig. 4(b). Since the low-temperature specific heat appears to be qualitatively equivalent even in magnetic fields, this behavior is considered to be robust against an applied magnetic field. The characteristic energy scale of the RS state, T_0, is evaluated to be approximately 11 K, which is in close agreement with the energy scale observed in the magnetization data.

V. SUMMARY

In this research, we synthesized a verdazyl-based complex: $[Cu_2(AcO)_4(p-Py-V-p-F)_2]\cdot 4CHCl_3$. The four bridging acetates and two *p*-Py-V-*p*-F ligands formed a distorted square pyramidal geometry around the Cu atoms, creating a paddlewheel structure. Strong AF exchange interactions between Cu spins generated a spin-1/2 AF dimer, stabilizing the nonmagnetic singlet state below ~100 K. We identified two primary exchange interactions between the radical spins, J_R and J_L, which generated a spin- 1/2 AF

two-leg ladder. Two possible positional configurations of the F atom lead to four different MO overlap configurations associated with J_R and J_L, introducing bond randomness in the spin ladder. The magnetic susceptibility indicated a broad peak with a Curie tail in the low-temperature region, indicating AF correlations and low paramagnetic contribution. The magnetization curve exhibited a gapless gradual increase up to ∼10 T, followed by a rapid rise toward spin-1/2 ladder saturation. The specific heat showed a broad, magnetic-field-insensitive peak, indicating the development of AF correlations, rather than a Schottky peak related to an energy gap. Furthermore, in the low-temperature region, the specific heat exhibited the $1/|\ln T|^3$ behavior predicted for the unfrustrated RS state. The observed experimental behaviors of the system were attributed to a wide distribution of excitation energies, with a few orphan spins in the RS state. In addition, the restricted patterns of exchange interactions and the one-dimensional nature of the system were considered to induce some deviations from the expected theoretical RS behavior. These findings provide insight into the effects of bond randomness on the quantum behavior of spin ladders. We propose a one-dimensional spin model of V-QOM with bond randomness. This development is expected to inspire further research into the quantum phenomena arising from the interplay of quantum fluctuations and randomness.

ACKNOWLEDGMENTS

This research was partly supported by KAKENHI (Grants No. 23K13065 and No. 23H01127) and the Iwatani Naoji Foundation. A part of this work was performed under the interuniversity cooperative research program of the joint-research program of ISSP, the University of Tokyo.

[1] E. Dagotto and T. M. Rice, Surprises on the way from one- to two-dimensional quantum magnets: The ladder materials, Science **271**, 618 (1996).

[2] M. Uehara, T. Nagata, J. Akimitsu, H. Takahashi, N. Môri, and K. Kinoshita, Superconductivity in the ladder material $Sr_{0.4}Ca_{13.6}Cu_{24}O_{41.84}$, J. Phys. Soc. Jpn. **65**, 2764 (1996).

[3] M. Azuma, Z. Hiroi, M. Takano, K. Ishida, and Y. Kitaoka, Observation of a spin gap in $SrCu_2O_3$ comprising spin-1/2 quasi-1D two-leg ladders, Phys. Rev. Lett. **73**, 3463 (1994).

[4] C. Rüegg, K. Kiefer, B. Thielemann, D. F. McMorrow, V. Zapf, B. Normand, M. B. Zvonarev, P. Bouillot, C. Kollath, T. Giamarchi, S. Capponi, D. Poilblanc, D. Biner, and K. W. Krämer, Thermodynamics of the spin Luttinger liquid in a model ladder material, Phys. Rev. Lett. **101**, 247202 (2008).

[5] B. Thielemann, C. Rüegg, H. M. Rø, A. M. Läuchli, J.-S. Caux, B. Normand, D. Biner, K. W. Krämer, H.-U. Güdel, J. Stahn, K. Habicht, K. Kiefer, M. Boehm, D. F. McMorrow, and J. Mesot, Direct observation of magnon fractionalization in the quantum spin ladder, Phys. Rev. Lett. **102**, 107204 (2009).

[6] T. Hong, Y. H. Kim, C. Hotta, Y. Takano, G. Tremelling, M. M. Turnbull, C. P. Landee, H.-J. Kang, N. B. Christensen, K. Lefmann, K. P. Schmidt, G. S. Uhrig, and C. Broholm, Field-induced Tomonaga-Luttinger liquid phase of a two-leg spin-1/2 ladder with strong leg interactions, Phys. Rev. Lett. **105**, 137207 (2010).

[7] C. Dasgupta and S.-K. Ma, Low-temperature properties of the random Heisenberg antiferromagnetic chain, Phys. Rev. B **22**, 1305 (1980).

[8] S.-K. Ma, C. Dasgupta, and C.-K. Hu, Random antiferromagnetic chain, Phys. Rev. Lett. **43**, 1434 (1979).

[9] J. E. Hirsch, Low-temperature thermodynamic properties of a random anisotropic antiferromagnetic chain, Phys. Rev. B **22**, 5355 (1980).

[10] D. S. Fisher, Random antiferromagnetic quantum spin chains, Phys. Rev. B **50**, 3799 (1994).

[11] K. Watanabe, H. Kawamura, H. Nakano, and T. Sakai, Quantum spin-liquid behavior in the spin-1/2 random Heisenberg antiferromagnet on the triangular lattice, J. Phys. Soc. Jpn. **83**, 034714 (2014).

[12] T. Shimokawa, K. Watanabe, and H. Kawamura, Static and dynamical spin correlations of the $S = 1/2$ random-bond antiferromagnetic Heisenberg model on the triangular and kagome lattices, Phys. Rev. B **92**, 134407 (2015).

[13] K. Uematsu and H. Kawamura, Randomness-induced quantum spin liquid behavior in the $S = 1/2$ random $J_1 - J_2$ Heisenberg antiferromagnet on the square lattice, Phys. Rev. B **98**, 134427 (2018).

[14] I. Kimchi, J. P. Sheckelton, T. M. McQueen, and P. A. Lee, Scaling and data collapse from local moments in frustrated disordered quantum spin systems, Nat. Commun. **9**, 4367 (2018).

[15] H. Kawamura and K. Uematsu, Nature of the randomness-induced quantum spin liquids in two dimensions, J. Phys.: Condens. Matter **31**, 504003 (2019).

[16] K. Uematsu, T. Hikihara, and H. Kawamura, Frustration-induced quantum spin liquid behavior in the $s = 1/2$ random-bond Heisenberg antiferromagnet on the zigzag chain, J. Phys. Soc. Jpn. **90**, 124703 (2021).

[17] J. Bobroff, N. Laflorencie, L. K. Alexander, A. V. Mahajan, B. Koteswararao, and P. Mendels, Impurity-induced magnetic order in low-dimensional spin-gapped materials, Phys. Rev. Lett. **103**, 047201 (2009).

[18] D. Schmidiger, K. Y. Povarov, S. Galeski, N. Reynolds, R. Bewley, T. Guidi, J. Ollivier, and A. Zheludev, Emergent interacting spin islands in a depleted strong-leg Heisenberg ladder, Phys. Rev. Lett. **116**, 257203 (2016).

[19] C. Pughe, O. H. J. Mustonen, A. S. Gibbs, S. Lee, R. Stewart, B. Gade, C. Wang, H. Luetkens, A. Foster, F. C. Coomer, H. Takagi, and E. J. Cussen, Partitioning the two-leg spin ladder in $Ba_2Cu_{1-x}Zn_xTeO_6$: From magnetic order through spin-freezing to paramagnetism, Chem. Mater. **35**, 2752 (2023).

[20] R. Mélin, Y.-C. Lin, P. Lajkó, H. Rieger, and F. Iglói, Strongly disordered spin ladders, Phys. Rev. B **65**, 104415 (2002).

[21] M. Hörmann, P. Wunderlich, and K. P. Schmidt, Dynamic structure factor of disordered quantum spin ladders, Phys. Rev. Lett. **121**, 167201 (2018).

[22] U. Kanbur, H. Polat, and E. Vatansever, Thermal properties of rung-disordered two-leg quantum spin ladders: Quantum Monte Carlo study, Phys. Rev. E **102**, 042104 (2020).

[23] H. Yamaguchi, K. Iwase, T. Ono, T. Shimokawa, H. Nakano, Y. Shimura, N. Kase, S. Kittaka, T. Sakakibara, T. Kawakami, and Y. Hosokoshi, Unconventional magnetic and thermodynamic properties of $S = 1/2$ spin ladder with ferromagnetic legs, Phys. Rev. Lett. **110**, 157205 (2013).

[24] H. Yamaguchi, Y. Tamekuni, Y. Iwasaki, and Y. Hosokoshi, Candidate for a fully frustrated square lattice in a Verdazyl-based salt, Phys. Rev. B **97**, 201109(R) (2018).

[25] H. Yamaguchi, Y. Sasaki, T. Okubo, M. Yoshida, T. Kida, M. Hagiwara, Y. Kono, S. Kittaka, T. Sakakibara, M. Takigawa, Y. Iwasaki, and Y. Hosokoshi, Field-enhanced quantum fluctuation in an $S = 1/2$ frustrated square lattice, Phys. Rev. B **98**, 094402 (2018).

[26] H. Yamaguchi, T. Okita, Y. Iwasaki, Y. Kono, N. Uemoto, Y. Hosokoshi, T. Kida, T. Kawakami, A. Matsuo, and M. Hagiwara, Experimental realization of Lieb-Mattis plateau in a quantum spin chain, Sci. Rep. **10**, 9193 (2020).

[27] H. Yamaguchi, Y. Iwasaki, Y. Kono, T. Okubo, S. Miyamoto, Y. Hosokoshi, A. Matsuo, T. Sakakibara, T. Kida, and M. Hagiwara, Quantum critical phenomena in a spin-1/2 frustrated square lattice with spatial anisotropy, Phys. Rev. B **103**, L220407 (2021).

[28] H. Yamaguchi, M. Okada, Y. Kono, S. Kittaka, T. Sakakibara, T. Okabe, Y. Iwasaki, and Y. Hosokoshi, Gapped ground state in a spin-1/2 frustrated square lattice, Sci. Rep. **7**, 16144 (2017).

[29] R. Kuhn, Über Verdazyle und verwandte Stickstoffradikale, Angew. Chem. **76**, 691 (1964).

[30] M. Shoji, K. Koizumi, Y. Kitagawa, T. Kawakami, S. Yamanaka, M. Okumura, and K. Yamaguchi, A general algorithm for calculation of Heisenberg exchange integrals J in multispin systems, Chem. Phys. Lett. **432**, 343 (2006).

[31] A. W. Sandvik, Stochastic series expansion method with operator-loop update, Phys. Rev. B **59**, R14157 (1999).

[32] A. F. Albuquerque, F. Alet, P. Corboz, P. Dayal, A. Feiguin, L. Gamper, E. Gull, S. Gurtler, A. Honecker, R. Igarashi, M. Korner, A. Kozhevnikov, A. Lauchli, S. R. Manmana, M. Matsumoto, I. P. McCulloch, F. Michel, R. M. Noack, G. Pawlowski, L. Pollet *et al.*, The ALPS project release 1.3: Open-source software for strongly correlated systems, J. Magn. Magn. Mater. **310**, 1187 (2007).

[33] B. Bauer, L. D. Carr, A. Feiguin, J. Freire, S. Fuchs, L. Gamper, J. Gukelberger, E. Gull, S. Guertler, A. Hehn, R. Igarashi, S. V. Isakov, D. Koop, P. N. Ma, P. Mates, H. Matsuo, O. Parcollet, G. Pawlowski, J. D. Picon, L. Pollet *et al.*, The ALPS project release 2.0: Open source software for strongly correlated systems, J. Stat. Mech.: Theory Exp. (2011) P05001.

[34] Viola, N. Muhammad, M. Ikram, S. Rehman, S. Ali, M. N. Akhtar, M. A. AlDamen, and C. Schulzke, A paddle wheel dinuclear Copper(II) carboxylate: Crystal structure, thermokinetic and magnetic properties, J. Mol. Struct. **1196**, 754 (2019).

[35] G. Psomas, Copper(II) and zinc(II) coordination compounds of non-steroidal anti-inflammatory drugs: Structural features and antioxidant activity, Coord. Chem. Rev. **412**, 213259 (2020).

[36] H. Yamaguchi, Y. Shinpuku, Y. Kono, S. Kittaka, T. Sakakibara, M. Hagiwara, T. Kawakami, K. Iwase, T. Ono, and Y. Hosokoshi, Unconventional $S = 2$ alternating chain realized by a metal-radical hybrid-spin approach, Phys. Rev. B **93**, 115145 (2016).

[37] S. Morota, T. Kida, M. Hagiwara, Y. Shimura, Y. Iwasaki, and H. Yamaguchi, Magnetic properties of a spin-1/2 octagonal lattice, Phys. Rev. B **109**, 054401 (2024).

[38] M. Barquín, N. Cocera, M. J. G. Garmendia, L. Larrínaga, E. Pinilla, and M. R. Torres, Acetato and formato copper(II) paddle-wheel complexes with nitrogen ligands, J. Coord. Chem. **63**, 2247 (2010).

[39] H. Li, H. Yao, E. Zhang, Y. Jia, H. Hou, and Y. Fan, Crystal structures and magnetism of infinite alternating chains arranged by paddle-wheel dinuclear copper and mononuclear copper units, Dalton Trans. **40**, 9388 (2011).

[40] J. Zhou, Z. Li, Y. Qiao, J. Liu, M. Zhu, P. Chem, and Q. Zhao, Synthesis, structure, and magnetic properties of two dimer paddle-wheel CuII toluate complexes with nitronyl nitroxide radicals, J. Coord. Chem. **66**, 2166 (2013).

[41] V. Paredes-García, R. Santana, R. Madrid, A. Vega, E. Spodine, and D. Venegas-Yazigi, Unusual conformation of a dinuclear paddle wheel copper(II) complex. Synthesis, structural characterization and EPR studies, Inorg. Chem. **52**, 8369 (2013).

[42] B. C. Watson, V. N. Kotov, M. W. Meisel, D. W. Hall, G. E. Granroth, W. T. Montfrooij, S. E. Nagler, D. A Jensen, R. Backov, M. A. Petruska, G. E. Fanucci, and D. R. Talham, Magnetic spin ladder $(C_5H_{12}N)_2CuBr_4$: High-field magnetization and scaling near quantum criticality, Phys. Rev. Lett. **86**, 5168 (2001).

[43] M. Ikeda, Z. Honda, M. Sakai, S. Kimura, K. Okunishi, and M. Hagiwara, High-field magnetization of the $S = 1/2$ two-leg spin-ladder antiferromagnets $CuAX_2$ (A = Diazine, X = Halogen), J. Low Temp. Phys. **170**, 296 (2013).

[44] H. Yamaguchi, H. Miyagai, M. Yoshida, M. Takigawa, K. Iwase, T. Ono, N. Kase, K. Araki, S. Kittaka, T. Sakakibara, T. Shimokawa, T. Okubo, K. Okunishi, A. Matsuo, and Y. Hosokoshi, Field-induced incommensurate phase in the strong-rung spin ladder with ferromagnetic legs, Phys. Rev. B **89**, 220402(R) (2014).

[45] H. Yamaguchi, S. C. Furuya, S. Morota, S. Shimono, T. Kawakami, Y. Kusanose, Y. Shimura, K. Nakano, and Y. Hosokoshi, Observation of thermodynamics originating from a mixed-spin ferromagnetic chain, Phys. Rev. B **106**, L100404 (2022).

[46] H. Yamaguchi, T. Okubo, K. Iwase, T. Ono, Y. Kono, S. Kittaka, T. Sakakibara, A. Matsuo, K. Kindo, and Y. Hosokoshi, Various regimes of quantum behavior in an S = 1/2 Heisenberg antiferromagnetic chain with fourfold periodicity, Phys. Rev. B **88**, 174410 (2013).

[47] T. Masuda, A. Zheludev, B. Grenier, S. Imai, K. Uchinokura, E. Ressouche, and S. Park, Cooperative ordering of gapped and gapless spin networks in $Cu_2Fe_2Ge_4O_{13}$, Phys. Rev. Lett. **93**, 077202 (2004).